01

Entanglement of a Jaynes–Cummings atom and two Tavis–Cummings atoms

© A.R. Bagrov, E.K. Bashkirov

Samara National Research University named after S.P. Korolev,
443086 Samara, Russia
e-mail:bashkirov.ek@ssau.ru

Received November 12, 2025
Revised November 12, 2025
Accepted November 12, 2025

We demonstrated an exact solution of the quantum Liouville equation for a model consisting of three identical two-level atoms (qubits) A, B and C, and two independent resonators. Qubit A is assumed to be trapped in the first ideal resonator, and the two remaining qubits B and C are trapped in the second high-Q resonator. All qubits resonantly interact with the corresponding mode of the quantized thermal electromagnetic field of the resonator. Entanglement is assumed between the qubits at the initial time. We focus our attention on biseparable and genuine entangled W- and GHZ-type qubit states. Based on the exact solution, the Peres-Horodecki criterion (negativity) and the fidelity are calculated. Using the specified entanglement criteria, the dynamics of two- and three-qubit entanglement are analyzed for various resonator thermal field intensities, and a comparative analysis of the qubit entanglement dynamics in the model under consideration is conducted with previously studied three-qubit models. It is shown that qubits never transit to initial states during their evolution, which fundamentally distinguishes their behavior from that of qubits in previously studied three-qubit models.

Keywords: qubits, genuine entangled W-type states and GHZ-states, biseparable states, thermal fields, entanglement, independent resonators, negativity, fidelity, quantum Liouville equation, sudden death of entanglement.

DOI: 10.61011/TP.2026.05.63511.313-25

Introduction

Entanglement or non-local quantum correlations between two (or more) quantum subsystems is one of the striking traits of quantum mechanics compared with classical mechanics. Recently, special attention has been paid to the study of entangled states due to their fundamental role in numerous applications such as quantum computing and communications, density coding, cryptography, etc. [1]. The most well-known entangled states, such as EPR states or Bell states, can be obtained in systems consisting of a pair of qubits. In recent years, such states for two-qubit systems of various physical nature have been investigated in a huge number of theoretical and experimental studies. In quantum information processing, the two-qubit systems play special role because all quantum algorithms can be expanded into a minimal universal set of gates consisting of one-qubit and two-qubit operations [2]. At the same time, the use of multiparticle entangled states makes it possible to implement more complex quantum algorithms, for example, to perform quantum calculations using universal three-qubit Toffoli and Fredkin gates [3,4], cluster states [5], to improve quantum error correction schemes [6] and others.

Since no quantum system exists in isolation, the interaction of entangled qubits with the environment leads to decoherence [7,8]. In systems used in quantum information processing, the time required to perform operations with qubits for any real-world quantum technology application should be less than the decay time of the qubits quantum nonlocal correlations [9]. This creates serious problems when using entanglement as an information resource. Under these conditions, it becomes necessary to fully understand the temporal dynamics of entanglement in multiqubit systems. To generate, maintain and control the entangled states of atomic qubits, their interaction with the electromagnetic fields of resonators is used [10–13]. In this regard, the platforms of resonators quantum electrodynamics (RQED), which are most convenient for experimental realization, are the most adequate devices for a detailed study of the dynamics of qubits interaction with electromagnetic fields [10–13]. Such platforms are themselves high-Q microwave or optical resonators in which qubits of various physical nature are embedded. For theoretical analysis of the dynamics of cubits entanglement in RQED the Jaynes–Cummings model (JCM) and its generalizations are used, in particular, the multiqubit Tavis–Cummings model (TCM) [14,15]. Difficulties in describing the dynamics of TCM models increase significantly with a higher number of qubits. Therefore, at present, special attention is paid to the analysis of the three-qubit models. Three-qubit quantum entangled states have been experimentally implemented in a series of tests in systems of superconducting qubits, trapped ions, and impurity spins [16–21]. The dynamics of qubits entanglement in various single- and multiphoton extensions of a three-qubit TCM for various initial states of qubits and resonator fields has been discussed in a number of articles (see reference in [22–25]).

In this paper, we investigated the exact dynamics of entanglement of three identical two-level atoms (qubits) in a new version of a three-atom TCM consisting of an atom trapped in an ideal single-mode resonator and two atoms embedded in another single-mode ideal common resonator. The atoms resonantly interact with the fields of resonators via single-photon processes. We have found an exact expression for the evolution operator of the considered triatomic model. Based on the exact solution, we investigated the dynamics of the considered quantum model for the initial biseparable and genuine entangled W- and GHZ-states of atoms, and thermal states as the initial states of the resonator fields. Pairwise negativity and fidelity were used as criteria for atomic entanglement. The choice of thermal states of resonator fields is determined by the presence of thermal photons in resonators of any RQED platforms. Due to the interaction of atoms with thermal fields of the resonators, Rabi oscillations of atoms entanglement parameters are possible, as well as the sudden death of atoms entanglement, i.e., the disappearance of entanglement at times shorter than the decoherence time. Such effects can lead to errors when reading information about the state of qubits. Therefore, the study of dynamics of atoms thermal entanglement in triatomic models is of undoubted interest for quantum computer science.

1. Description of a three-qubit model and exact solution of the Liouville quantum equation

Let's describe the quantum model of interest. We consider three two-level atoms (qubits) A, B and C. A qubit is trapped in the first ideal resonator, and B and C qubits are trapped in a similar high-Q second resonator. All three qubits resonantly interact with the corresponding selected mode of their thermal quantum electromagnetic field of the resonator through single-photon processes. For simplicity, let's assume that the interaction constants of the qubits with the corresponding resonator field modes are $\gamma_A = \gamma_B = \gamma_C \equiv \gamma$. The scheme of the considered model is shown in Fig. 1.

The Hamiltonian of interaction $\hat{H}_{Int}$ of the given model can be represented in standard approximations in the following form:

$$\hat{H}_{Int}=\hbar\gamma\left(\hat{\sigma}_A^+\hat{a}_1+\hat{\sigma}_A^-\hat{a}_1^+ +\hat{\sigma}_B^+\hat{a}_2+\hat{\sigma}_B^-\hat{a}_2^+ +\hat{\sigma}_C^+\hat{a}_2+\hat{\sigma}_C^-\hat{a}_2^+\right), \tag{1}$$

where classical notations for the quantum optics $\hat{\sigma}_i^+ = |+\rangle_{ii}\langle-|$ and $\hat{\sigma}_i^- = |-\rangle_{ii}\langle+|$ are introduced — raising and lowering operators in i-th qubit ($i = A, B, C$), $\hat{a}_1(\hat{a}_2)$ and $\hat{a}_1^+(\hat{a}_2^+)$ — are operators of the annihilation and creation of photons in the mode of the first (second) resonator.

Before investigating the interaction of A, B, and C qubits with the corresponding modes of the resonator thermal fields, we study the system dynamics for the Fock initial states of the resonator fields, i.e. for states with a certain number of particles. To find the wave function at subsequent time points $t > 0$ in the case of the Fock states of the resonator fields, it is convenient to introduce a new parameter N to determine the basis of the Hilbert space where the system evolution will take place. This parameter is introduced as follows: $N = N_1 + N_2$, where

$$N_1 = \begin{cases} 0, & \text{if } n_{q_A} = n_1 = 0, \\ 1, & \text{if } n_{q_A} = 0, n_1 \geq 1 \text{ or } n_{q_A} = 1, n_1 \geq 0, \end{cases}$$

$$N_2 = \begin{cases} 0, & \text{if } n_{q_{B+C}} = n_2 = 0, \\ 1, & \text{if } n_{q_{B+C}} = 1, n_2 = 0 \text{ or } n_{q_{B+C}} = 0, n_2 = 1, \\ 2, & \text{if } n_{q_{B+C}} = 2, n_2 \geq 0 \text{ or } n_{q_{B+C}} = 1, n_2 \geq 1, \\ & \text{or } n_{q_{B+C}} = 0, n_2 \geq 2, \end{cases}$$

where n_{q_A} — number of excited qubits in the first resonator, $n_{q_{B+C}} = n_{q_B} + n_{q_C}$ — number of excited qubits in the second resonator, $n_1(n_2)$ — number of photons in the mode of the first (second) resonator. Therefore, the parameter N may take the following values: 0, 1, 2 and 3.

If the parameter takes the value $N = 3$, then the evolution of the system state vector takes place in an 8-dimensional Hilbert space, and it is convenient to represent this basic set in the following form:

$$\begin{gathered} |+,+,+,n_1,n_2\rangle, |+,+,-,n_1,n_2+1\rangle, \\ |+,-,+,n_1,n_2+1\rangle, |-,+,+,n_1+1,n_2\rangle, \\ |+,-,-,n_1,n_2+2\rangle, |-,+,-,n_1+1,n_2+1\rangle, \\ |-,-,+,n_1+1,n_2+1\rangle, |-,-,-,n_1+1,n_2+2\rangle. \end{gathered} \tag{2}$$

Here and further in our work, we will use a simplified mathematical notation for the ket vectors of the subsystem of three qubits $|x,y,z\rangle \equiv |x_A, y_B, z_C\rangle \equiv |x_A\rangle \otimes |y_B\rangle \otimes |z_C\rangle$ and for the ket vectors of the complete system $|x,y,z,n_1,n_2\rangle \equiv |x_A, y_B, z_C, n_1, n_2\rangle \equiv |x_A\rangle \otimes |y_B\rangle \otimes |z_C\rangle \otimes |n_1\rangle \otimes |n_2\rangle$, where $x_i, y_i, z_i = +_i, -_i$. In case of $N = 2$, there are two sets of basis vectors due to differences in the evolution of different qubits in the resonators. Either the following set of parameters $N_1 = 1, N_2 = 1$ is possible that is, when the evolution of the state vector occurs in a 6-dimensional Hilbert space:

$$\begin{gathered} |+,+,-,n_1,0\rangle, |+,-,+,n_1,0\rangle, \\ |+,-,-,n_1,1\rangle, |-,+,-,n_1+1,0\rangle, \\ |-,-,+,n_1+1,0\rangle, |-,-,-,n_1+1,1\rangle, \end{gathered} \tag{3}$$

either a set of parameters $N_1 = 0, N_2 = 2$, and then the evolution of the state vector occurs in a 4-dimensional Hilbert space:

$$\begin{gathered} |-,+,+,0,n_2\rangle, |-,+,-,0,n_2+1\rangle, \\ |-,-,+,0,n_2+1\rangle, |-,-,-,0,n_2+2\rangle. \end{gathered} \tag{4}$$

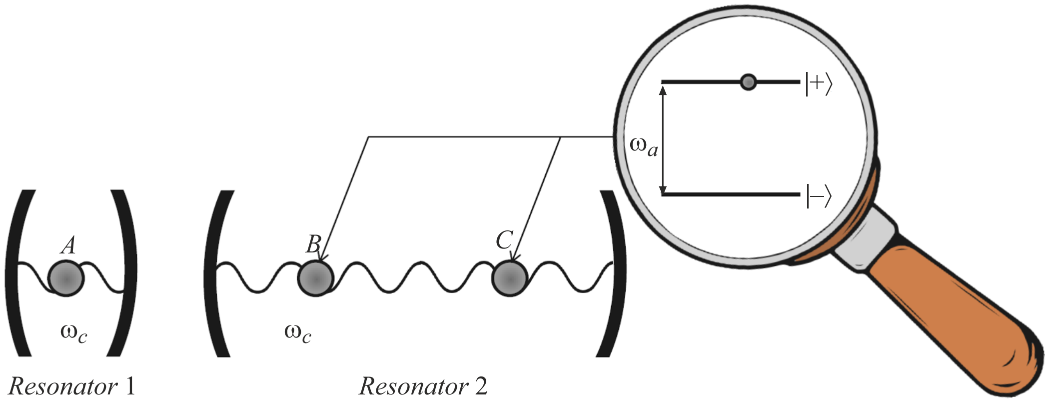

Figure 1. Configuration of the studied model. Here ω_c — resonator frequency, $\omega_a = \omega_c$ — transition frequency in the qubit between the excited $|+\rangle$ and ground $|-\rangle$ levels.

In case of $N = 1$ two sets of the basic vectors exist. Or $N_1 = 1, N_2 = 0$, and then it is convenient to represent the set of basis vectors in the following form:

$$|+,-,-,n_1,0\rangle, |-,-,-,n_1+1\rangle, \tag{5}$$

Or $N_1 = 0, N_2 = 1$, and then it is convenient to represent the set of basis vectors in the following form:

$$|-,+,-,0,0\rangle, |-,-,+,0,0\rangle, |-,-,-,0,1\rangle. \tag{6}$$

In case of $N = 3$, we have obtained an exact solution to the nonstationary Schrodinger equation in the basic set (2) for the studied model with the interaction Hamiltonian (1). We provide an exact compact solution as an evolution operator $\hat{U}$ in the basic set (2) as:

$$\hat{U} = \begin{pmatrix} U_{11} & U_{12} & U_{13} & U_{14} & U_{15} & U_{16} & U_{17} & U_{18} \\ U_{21} & U_{22} & U_{23} & U_{24} & U_{25} & U_{26} & U_{27} & U_{28} \\ U_{31} & U_{32} & U_{33} & U_{34} & U_{35} & U_{36} & U_{37} & U_{38} \\ U_{41} & U_{42} & U_{43} & U_{44} & U_{45} & U_{46} & U_{47} & U_{48} \\ U_{51} & U_{52} & U_{53} & U_{54} & U_{55} & U_{56} & U_{57} & U_{58} \\ U_{61} & U_{62} & U_{63} & U_{64} & U_{65} & U_{66} & U_{67} & U_{68} \\ U_{71} & U_{72} & U_{73} & U_{74} & U_{75} & U_{76} & U_{77} & U_{78} \\ U_{81} & U_{82} & U_{83} & U_{84} & U_{85} & U_{86} & U_{87} & U_{88} \end{pmatrix},$$

$$\begin{pmatrix} |+,+,+,n_1,n_2\rangle \\ |+,+,-,n_1,n_2+1\rangle \\ |+,-,+,n_1,n_2+1\rangle \\ |-,+,+,n_1+1,n_2\rangle \\ |+,-,-,n_1,n_2+2\rangle \\ |-,+,-,n_1+1,n_2+1\rangle \\ |-,-,+,n_1+1,n_2+1\rangle \\ |-,-,-,n_1+1,n_2+2\rangle \end{pmatrix}, \tag{7}$$

where the elements of the evolution operator $U_{ij} \equiv U_{ij}(n_1, n_2, t)$ are specified by the following expressions:

$$U_{11} = \begin{cases} \frac{\cos\left(\gamma t\sqrt{4n_2+6}\right)\left[n_2+2+(n_2+1)\cos\left(\gamma t\sqrt{4n_2+6}\right)\right]}{2n_2+3}, \\ \qquad \text{if } n_1 = 4n_2+5 \\ \frac{2(n_2+2)\cos(\gamma t\sqrt{n_1+1})+(n_2+1)[\cos(\gamma\theta_2 t)+\cos(\gamma\theta_1 t)]}{4n_2+6}, \\ \qquad \text{else} \end{cases}$$

$$U_{22} = \begin{cases} \cos^2(\gamma t\sqrt{n_2+3/2})\cos(\gamma t\sqrt{4n_2+6}), & \text{if } n_1 = 4n_2+5 \\ \frac{1}{4}\left[2\cos\left(\gamma t\sqrt{n_1+1}\right) + \cos\left(\gamma t\theta_2\right) + \cos\left(\gamma t\theta_1\right)\right], & \text{else} \end{cases}$$

$$U_{55} = \begin{cases} \frac{\cos\left(\gamma t\sqrt{4n_2+6}\right)\left[n_2+1+(n_2+2)\cos\left(\gamma t\sqrt{4n_2+6}\right)\right]}{2n_2+3}, & \text{if } n_1 = 4n_2+5 \\ \frac{2(n_2+1)\cos\left(\gamma t\sqrt{n_1+1}\right)+(n_2+2)[\cos(\gamma t\theta_2)+\cos(\gamma t\theta_1)]}{4n_2+6}, & \text{else} \end{cases}$$

$$U_{21} = \begin{cases} -\frac{\mathrm{i}\sqrt{n_2+1}}{2\sqrt{4n_2+6}}\sin\left(2\gamma t\sqrt{4n_2+6}\right), & \text{if } n_1 = 4n_2+5 \\ -\frac{\mathrm{i}}{8n_2+12}\sqrt{\frac{n_2+1}{(n_1-4n_2-5)^2}}\left[\theta_1(4n_2+6-\alpha)\sin\left(\gamma\theta_2 t\right) \right. \\ \qquad \left. +\theta_2(4n_2+6+\alpha)\sin\left(\gamma\theta_1 t\right)\right], & \text{else} \end{cases}$$

$$U_{41} = \begin{cases} -\frac{\mathrm{i}}{2n_2+3}\left[n_2+2+(n_2+1)\cos\left(\gamma t\sqrt{4n_2+6}\right)\right] \\ \times\sin(\gamma t\sqrt{4n_2+6}), \quad \text{if } n_1 = 4n_2+5 \\ -\frac{\mathrm{i}}{2(2n_2+3)}\left[2(n_2+2)\sin(\gamma t\sqrt{n_1+1}) - (n_2+1) \right. \\ \left. \times\left(\frac{\theta_1\beta_1\sin(\gamma\theta_2 t)+\theta_2\beta_2\sin(\gamma\theta_1 t)}{\chi}\right)\right], \quad \text{else} \end{cases}$$

$$U_{85} = \begin{cases} -\frac{\mathrm{i}}{2n_2+3}\left[n_2+1+(n_2+2)\cos\left(\gamma t\sqrt{4n_2+6}\right)\right] \\ \quad \times\sin(\gamma t\sqrt{4n_2+6}), \quad \text{if } n_1 = 4n_2+5 \\ -\frac{\mathrm{i}}{2(2n_2+3)}\left[2(n_2+1)\sin(\gamma t\sqrt{n_1+1}) - (n_2+2) \right. \\ \quad \left. \times\left(\frac{\theta_1\beta_1\sin(\gamma\theta_2 t)+\theta_2\beta_2\sin(\gamma\theta_1 t)}{\chi}\right)\right], \quad \text{else} \end{cases}$$

$$U_{51} = \begin{cases} -\frac{2\sqrt{(n_2+1)(n_2+2)}}{2n_2+3}\cos(\gamma t\sqrt{4n_2+6})\sin^2(\gamma t\sqrt{n_2+3/2}), \\ \text{if } n_1 = 4n_2+5 \\ \frac{\sqrt{(n_2+1)(n_2+2)}}{4n_2+6}\left[\cos(\gamma\theta_1 t) + \cos(\gamma\theta_2 t) \right. \\ \left. -2\cos(\gamma t\sqrt{n_1+1})\right], \quad \text{else} \end{cases}$$

$$U_{61} = \begin{cases} -\frac{\sqrt{n_2+1}}{\sqrt{4n_2+6}} \sin^2(\gamma t\sqrt{4n_2+6}), \quad \text{if } n_1 = 4n_2+5 \\ \frac{1}{2}\sqrt{\frac{n_2+1}{4n_2+6}}(\cos(\gamma\theta_1 t) - \cos(\gamma\theta_2 t)), \ \text{else} \end{cases}$$

$$U_{81} = \begin{cases} \frac{2\mathrm{i}\sqrt{(n_2+1)(n_2+2)}}{2n_2+3} \sin(\gamma t\sqrt{4n_2+6}) \sin^2(\gamma t\sqrt{n_2+3/2}), \\ \quad \text{if } n_1 = 4n_2+5 \\ \frac{\mathrm{i}\sqrt{(n_2+1)(n_2+2)}}{2(2n_2+3)} \Big[2\sin(\gamma t\sqrt{n_1+1}) + \frac{(\alpha-n_1-1)\sin(\gamma\theta_2 t)}{\theta_2\sqrt{n_1+1}} \\ -\frac{(\alpha+n_1+1)\sin(\gamma\theta_1 t)}{\theta_1\sqrt{n_1+1}} \Big], \ \text{else} \end{cases}$$

$$U_{32} = \begin{cases} -\cos(\gamma t\sqrt{4n_2+6}) \sin^2\left(\gamma t\sqrt{n_2+3/2}\right), \\ \qquad \text{if } n_1 = 4n_2+5 \\ \frac{1}{4}\Big[\cos(\gamma\theta_1 t) + \cos(\gamma\theta_2 t) - 2\cos(\gamma t\sqrt{n_1+1})\Big], \\ \qquad \text{else} \end{cases}$$

$$U_{52} = \begin{cases} -\frac{\mathrm{i}\sqrt{n_2+2}}{2\sqrt{4n_2+6}} \sin(2\gamma t\sqrt{4n_2+6}), \quad \text{if } n_1 = 4n_2+5 \\ -\frac{\mathrm{i}}{8n_2+12}\sqrt{\frac{n_2+2}{(n_1-4n_2-5)^2}} \left[\theta_1(4n_2+6-\alpha)\sin(\gamma\theta_2 t) \right. \\ \quad \left. +\, \theta_2(4n_2+6+\alpha)\sin(\gamma\theta_1 t)\right], \ \text{else} \end{cases}$$

$$U_{62} = \begin{cases} -2\mathrm{i}\cos^3\left(\gamma t\sqrt{n_2+3/2}\right)\sin\left(\gamma t\sqrt{n_2+3/2}\right), \\ \qquad \text{if } n_1 = 4n_2+5 \\ -\frac{\mathrm{i}}{4}\Big[2\sin(\gamma t\sqrt{n_1+1}) + \frac{(n_1-\alpha+1)\sin(\gamma\theta_2 t)}{\theta_2\sqrt{n_1+1}} \\ \qquad + \frac{(n_1+\alpha+1)\sin(\gamma\theta_1 t)}{\theta_1\sqrt{n_1+1}}\Big], \ \text{else} \end{cases}$$

$$U_{72} = \begin{cases} \mathrm{i}\sin^2(\gamma t\sqrt{n_2+3/2})\sin\left(\gamma t\sqrt{4n_2+6}\right), \\ \qquad \text{if } n_1 = 4n_2+5 \\ \frac{\mathrm{i}}{4}\Big[2\sin(\gamma t\sqrt{n_1+1}) + \frac{(\alpha-n_1-1)\sin(\gamma\theta_2 t)}{\theta_2\sqrt{n_1+1}} \\ \qquad - \frac{(\alpha+n_1+1)\sin(\gamma\theta_1 t)}{\theta_1\sqrt{n_1+1}}\Big], \ \text{else} \end{cases}$$

$$U_{82} = \begin{cases} -\frac{\sqrt{n_2+2}}{\sqrt{4n_2+6}} \sin^2(\gamma t\sqrt{4n_2+6}), \quad \text{if } n_1 = 4n_2+5 \\ \frac{1}{2}\sqrt{\frac{n_2+2}{4n_2+6}}\left[\cos(\gamma\theta_1 t) - \cos(\gamma\theta_2 t)\right], \ \text{else,} \end{cases}$$

where the following notations are provided to save the space:

$$\theta_1 = \sqrt{7+n_1+4n_2+\Omega}, \ \theta_2 = \sqrt{7+n_1+4n_2-\Omega},$$

$$\Omega = 2\alpha, \quad \alpha = \sqrt{2(n_1+1)(2n_2+3)},$$

$$\chi = \sqrt{(n_1+1)(n_1-4n_2-5)^2}\Big[49 + 4n_1^2 - 10\Omega$$
$$+ n_1(44+24n_2-4\Omega) + 4n_2(9+n_2-\Omega)\Big],$$

$$\beta_1 = -169 - 4n_1^3 + \frac{69}{2}\Omega - 4n_1n_2(55+9n_2-4\Omega)$$
$$+ 4n_1^2\left(-24-14n_2+\frac{3}{2}\Omega\right) + 9n_1(-29+4\Omega)$$
$$+ 4n_2\left(-41+\frac{11}{2}\Omega + n_2\left(\frac{\Omega}{2}-9\right)\right),$$

$$\beta_2 = 71 - 4n_1^3 - \frac{29}{2}\Omega + 2n_1^2(4n_2+\Omega)$$
$$- 2n_2(-46-14n_2+7\Omega+n_2\Omega)$$
$$+ n_1\big(75 - 8\Omega + 4n_2(25+7n_2-2\Omega)\big),$$

and between the elements of the evolution operator U_{ij} the following ratios are valid:

$$U_{12} = U_{21} = U_{13} = U_{31} = U_{46} = U_{64} = U_{47} = U_{74},$$
$$U_{22} = U_{33} = U_{66} = U_{77},$$
$$U_{16} = U_{61} = U_{17} = U_{71} = U_{24} = U_{34} = U_{42} = U_{43},$$
$$U_{27} = U_{36} = U_{63} = U_{72},$$
$$U_{25} = U_{52} = U_{35} = U_{53} = U_{68} = U_{86} = U_{78} = U_{87},$$
$$U_{18} = U_{81} = U_{45} = U_{54},$$
$$U_{28} = U_{82} = U_{38} = U_{83} = U_{56} = U_{65} = U_{57} = U_{75},$$
$$U_{26} = U_{62} = U_{37} = U_{73}, \ U_{15} = U_{51} = U_{48} = U_{84},$$
$$U_{14} = U_{41}, \ U_{58} = U_{85}, \ U_{23} = U_{32} = U_{67} = U_{76},$$
$$U_{11} = U_{44}, \quad U_{55} = U_{88}.$$

In case of $N = 2$ the evolution operator $\hat{V}$ was obtained in the basic sets (3), (4):

$$\hat{V} = \begin{pmatrix} V_{11} & V_{12} & V_{13} & V_{14} & V_{15} & V_{16} & 0 & 0 & 0 & 0 \\ V_{21} & V_{22} & V_{23} & V_{24} & V_{25} & V_{26} & 0 & 0 & 0 & 0 \\ V_{31} & V_{32} & V_{33} & V_{34} & V_{35} & V_{36} & 0 & 0 & 0 & 0 \\ V_{41} & V_{42} & V_{43} & V_{44} & V_{45} & V_{46} & 0 & 0 & 0 & 0 \\ V_{51} & V_{52} & V_{53} & V_{54} & V_{55} & V_{56} & 0 & 0 & 0 & 0 \\ V_{61} & V_{62} & V_{63} & V_{64} & V_{65} & V_{66} & 0 & 0 & 0 & 0 \\ 0 & 0 & 0 & 0 & 0 & 0 & V_{77} & V_{78} & V_{79} & V_{7,10} \\ 0 & 0 & 0 & 0 & 0 & 0 & V_{87} & V_{88} & V_{89} & V_{8,10} \\ 0 & 0 & 0 & 0 & 0 & 0 & V_{97} & V_{98} & V_{99} & V_{9,10} \\ 0 & 0 & 0 & 0 & 0 & 0 & V_{10,7} & V_{10,8} & V_{10,9} & V_{10,10} \end{pmatrix},$$

$$\begin{pmatrix} |+,+,-,n_1,0\rangle \\ |+,-,+,n_1,0\rangle \\ |+,-,-,n_1,1\rangle \\ |-,+,-,n_1+1,0\rangle \\ |-,-,+,n_1+1,0\rangle \\ |-,-,-,n_1+1,1\rangle \\ |-,+,+,0,n_2\rangle \\ |-,+,-,0,n_2+1\rangle \\ |-,-,+,0,n_2+1\rangle \\ |-,-,-,0,n_2+2\rangle \end{pmatrix}, \qquad (8)$$

where the elements of the evolution operator $V_{ij} = V_{ij}(n_1, t)$ $(i, j = 1, \ldots 6)$, $V_{kl} = V_{kl}(n_2, t)$ $(k, l = 7, \ldots 10)$:

$$V_{11} = \begin{cases} \cos^2(\gamma t/\sqrt{2})\cos(\sqrt{2}\gamma t), \quad \text{if } n_1 = 1 \\ \frac{1}{4}\left[2\cos(\gamma t\sqrt{n_1+1}) + \cos(\gamma\alpha_2 t) + \cos(\gamma\alpha_1 t)\right], \ \text{else} \end{cases}$$

$$V_{33}=\begin{cases}\cos^2(\sqrt{2}\gamma t), & \text{if } n_1=1\\ \frac{1}{2}\left[\cos(\gamma\alpha_2 t)+\cos(\gamma\alpha_1 t)\right], & \text{else}\end{cases}$$

$$V_{21}=\begin{cases}-\cos(\sqrt{2}\gamma t)\sin^2\left(\gamma t/\sqrt{2}\right), & \text{if } n_1=1\\ \frac{1}{4}\left[\cos(\gamma\alpha_2 t)+\cos(\gamma\alpha_1 t)-2\cos(\gamma t\sqrt{n_1+1})\right], & \text{else}\end{cases}$$

$$V_{31}=\begin{cases}-\mathrm{i}\sin(2\sqrt{2}\gamma t)/2\sqrt{2}, & \text{if } n_1=1\\ \mathrm{i}\Big[\frac{\left(\sqrt{2}n_1-2\sqrt{n_1+1}+\sqrt{2}\right)\sin(\gamma\alpha_2 t)}{4\alpha_2\sqrt{n_1+1}} \\ \quad -\frac{\left(\sqrt{2}n_1+2\sqrt{n_1+1}+\sqrt{2}\right)\sin(\gamma\alpha_1 t)}{4\alpha_1\sqrt{n_1+1}}\Big], & \text{else}\end{cases}$$

$$V_{41}=\begin{cases}-2\mathrm{i}\cos^3\left(\gamma t/\sqrt{2}\right)\sin\left(\gamma t/\sqrt{2}\right), & \text{if } n_1=1\\ -\frac{\mathrm{i}}{4}\Big[2\sin(\gamma t\sqrt{n_1+1})+\frac{\left(n_1-\sqrt{2(n_1+1)}+1\right)\sin(\gamma\alpha_2 t)}{\alpha_2\sqrt{n_1+1}} \\ \quad +\frac{\left(n_1+\sqrt{2(n_1+1)}+1\right)\sin(\gamma\alpha_1 t)}{\alpha_1\sqrt{n_1+1}}\Big], & \text{else}\end{cases}$$

$$V_{51}=\begin{cases}\mathrm{i}\sin^2\left(\gamma t/\sqrt{2}\right)\sin(\sqrt{2}\gamma t), & \text{if } n_1=1\\ \frac{\mathrm{i}}{4}\Big[2\sin(\gamma t\sqrt{n_1+1})+\frac{\left(\sqrt{2(n_1+1)}-n_1-1\right)\sin(\gamma\alpha_2 t)}{\alpha_2\sqrt{n_1+1}} \\ \quad -\frac{\left(\sqrt{2(n_1+1)}+n_1+1\right)\sin(\gamma\alpha_1 t)}{\alpha_1\sqrt{n_1+1}}\Big], & \text{else}\end{cases}$$

$$V_{63}=\begin{cases}-\frac{\mathrm{i}}{2}\sin\left(2\sqrt{2}\gamma t\right), & \text{if } n_1=1\\ \mathrm{i}\Big[\frac{\left(\sqrt{2(n_1+1)}-n_1-1\right)\sin(\gamma\alpha_2 t)}{2\alpha_2\sqrt{n_1+1}} \\ \quad -\frac{\left(\sqrt{2(n_1+1)}+n_1+1\right)\sin(\gamma\alpha_1 t)}{2\alpha_1\sqrt{n_1+1}}\Big], & \text{else}\end{cases}$$

$$V_{77}=\frac{n_2+2+(n_2+1)\cos(\gamma t\sqrt{4n_2+6})}{2n_2+3},$$

$$V_{87}=-\mathrm{i}\sqrt{\frac{n_2+1}{4n_2+6}}\sin(\gamma t\sqrt{4n_2+6}),$$

$$V_{10,7}=-\frac{2\sqrt{(n_2+1)(n_2+2)}\sin^2\left(\gamma t\sqrt{n_2+3/2}\right)}{2n_2+3},$$

$$V_{88}=\cos^2(\gamma t\sqrt{n_2+3/2}),\ V_{98}=-\sin^2(\gamma t\sqrt{n_2+3/2}),$$

$$V_{10,8}=\frac{\sin\left(\gamma t\sqrt{4n_2+6}\right)}{\sqrt{\frac{2}{n_2+2}-4}},$$

$$V_{10,10}=\frac{n_2+1+(n_2+2)\cos\left(\gamma t\sqrt{4n_2+6}\right)}{2n_2+3},$$

and the following ratios between the elements of the evolution operator are true:

$$V_{11}=V_{22}=V_{44}=V_{55},\ V_{12}=V_{21}=V_{45}=V_{54},$$

$$V_{31}=V_{13}=V_{32}=V_{23}=V_{65}=V_{56}=V_{46}=V_{64},$$

$$V_{41}=V_{14}=V_{25}=V_{52},\ V_{51}=V_{15}=V_{42}=V_{24},$$

$$V_{61}=V_{16}=V_{43}=V_{34}=V_{53}=V_{35}=V_{62}=V_{26},$$

$$V_{87}=V_{78}=V_{97}=V_{79},\ V_{10,8}=V_{8,10}=V_{10,9}=V_{9,10},$$

$$V_{33}=V_{66},\ V_{63}=V_{36},\ V_{7,10}=V_{10,7},$$

$$V_{88}=V_{99},\quad V_{98}=V_{89},$$

where the following variables are introduced:

$$\alpha_1=\sqrt{3+n_1+2\sqrt{2(n_1+1)}},$$

$$\alpha_2=\sqrt{3+n_1-2\sqrt{2(n_1+1)}}.$$

If $N=1$ the evolution operator $\hat{S}$ was obtained in the basic sets (5), (6)

$$\hat{S}=\begin{pmatrix}S_{11}&S_{12}&0&0&0\\ S_{21}&S_{22}&0&0&0\\ 0&0&S_{33}&S_{34}&S_{35}\\ 0&0&S_{43}&S_{44}&S_{45}\\ 0&0&S_{53}&S_{54}&S_{55}\end{pmatrix},\ \begin{pmatrix}|+,-,-,n_1,0\rangle\\ |-,-,-,n_1+1,0\rangle\\ |-,+,-,0,0\rangle\\ |-,-,+,0,0\rangle\\ |-,-,-,0,1\rangle\end{pmatrix},\tag{9}$$

where the elements of the evolution operator S_{ij} are specified by the following expressions:

$$S_{11}(n_1,t)=\cos(\gamma t\sqrt{n_1+1}),$$

$$S_{21}(n_1,t)=-\mathrm{i}\sin(\gamma t\sqrt{n_1+1}),$$

$$S_{33}(t)=\cos^2(\gamma t/\sqrt{2}),\ S_{43}(t)=-\sin^2(\gamma t/\sqrt{2}),$$

$$S_{53}(t)=-\mathrm{i}\sin(\sqrt{2}\gamma t)/\sqrt{2}, S_{55}(t)=\cos(\sqrt{2}\gamma t),$$

given the ratios: $S_{11}=S_{22}$, $S_{12}=S_{21}$, $S_{43}=S_{34}$, $S_{33}=S_{44}$, $S_{35}=S_{45}=S_{53}=S_{54}$.

If $N=0$ no system evolution occurs. Thus, thanks to the evolution operators (7)–(9) we can find the wave function of the complete system $|\psi_{n_1n_2}(t)\rangle$ „three qubits + two modes of the resonator fields“ at subsequent time points t for any initial state of the qubits $|\psi(0)\rangle_{ABC}$ as follows:

$$|\psi_{n_1n_2}(t)\rangle=\hat{Q}\Big(|\psi(0)\rangle_{ABC}\otimes|n_1\rangle\otimes|n_2\rangle\Big),$$

where $\hat{Q}$ one of the evolution operators (7)–(9).

Note that the evolution operator of the considered system can be initially represented as a tensor product of the evolution operators of two subsystems. However, the approach used to write the full evolution operator makes it easier to calculate the entanglement criteria for the thermal fields of resonators.

Let's consider only the initial states of the two types of qubits. In the first case at the initial moment of time $t=0$ the atoms are prepared in such a biseparable state, that A and B are in the entangled Bell state $\cos\alpha|+,-\rangle+\sin\alpha|-,+\rangle$, and atom C is either in excited state $|+\rangle$, or in the ground state $|-\rangle$ ($\pi/2>\alpha>0$ — parameter stetting the initial degree of entanglement between A and B qubits). Then the initial state vector of the three qubits in this case will be written as follows:

$$|\psi_1(0)\rangle_{ABC}=\cos\alpha|+,-,-\rangle+\sin\alpha|-,+,-\rangle,\tag{10}$$

$$|\psi_2(0)\rangle_{ABC}=\cos\alpha|+,-,+\rangle+\sin\alpha|-,+,+\rangle.\tag{11}$$

In the second case, the atoms are initially prepared in genuine entangled W-type states

$$|W_1(0)\rangle_{ABC} = \cos\theta|+,+,-\rangle + \sin\theta\sin\varphi|+,-,+\rangle + \sin\theta\cos\varphi|-,+,+\rangle, \quad (12)$$

$$|W_2(0)\rangle_{ABC} = \cos\theta|-,-,+\rangle + \sin\theta\sin\varphi|-,+,-\rangle + \sin\theta\cos\varphi|+,-,-\rangle, \quad (13)$$

or GHZ-type state

$$|G(0)\rangle_{ABC} = \cos\vartheta|+,+,+\rangle + \sin\vartheta|-,-,-\rangle, \quad (14)$$

where θ, φ and ϑ — parameters in the range $(0, \pi/2)$, specifying the initial state of entanglement of A, B and C qubits.

Using the explicit form of the evolution operators (7)–(9), we have found exact solutions of the quantum Schrödinger equation for the initial states of qubits (10)–(14) and various Fock states of resonator fields. As an example, we give an explicit form of the time wave function $|\psi_{n_1n_2}(t)\rangle$ for the biseparable initial state of qubits (10):

1) Case $n_1 = n_2 = 0$ $(S_{i1} = S_{i1}(0,t), S_{i3} = S_{i3}(t))$:

$$|\psi_{0_10_2}(t)\rangle = \cos\alpha\Big[S_{11}|+,-,-,0,0\rangle + S_{21}|-,-,-,1,0\rangle\Big] + \sin\alpha\Big[S_{33}|-,+,-,0,0\rangle + S_{43}|-,-,+,0,0\rangle + S_{53}|-,-,-,0,1\rangle\Big].$$

2) Case $n_1 = 0, n_2 = 1$ $(V_{ij} = V_{ij}(0,t))$:

$$|\psi_{0_11_2}(t)\rangle = \cos\alpha\Big[V_{13}|+,+,-,0,0\rangle + V_{23}|+,-,+,0,0\rangle + V_{33}|+,-,-,0,1\rangle + V_{43}|-,+,-,1,0\rangle + V_{53}|-,-,+,1,0\rangle + V_{63}|-,-,-,1,1\rangle\Big] + \sin\alpha\Big[V_{78}|-,+,+,0,0\rangle + V_{88}|-,+,-,0,1\rangle + V_{98}|-,-,+,0,1\rangle + V_{10,8}|-,-,-,0,2\rangle\Big].$$

3) Case $n_1 \geq 1$, $n_2 = 0$ $(S_{ij} = S_{ij}(n_1,t), V_{ij} = V_{ij}(n_1-1,t))$:

$$|\psi_{n_10_2}(t)\rangle = \cos\alpha\big[S_{11}|+,-,-,n_1,0\rangle + S_{21}|-,-,-,n_1+1,0\rangle\big] + \sin\alpha\Big[V_{14}|+,+,-,n_1-1,0\rangle + V_{24}|+,-,+,n_1-1,0\rangle + V_{34}|+,-,-,n_1-1,1\rangle + V_{44}|-,+,-,n_1,0\rangle + V_{54}|-,-,+,n_1,0\rangle + V_{64}|-,-,-,n_1,1\rangle\Big].$$

4) Case $n_1 \geq 1$, $n_2 = 1$ $(V_{ij} = V_{ij}(n_1,t), U_{ij} = U_{ij}(n_1-1,0,t))$:

$$|\psi_{n_11_2}(t)\rangle = \cos\alpha\Big[V_{13}|+,+,-,n_1,0\rangle + V_{23}|+,-,+,n_1,0\rangle + V_{33}|+,-,-,n_1,1\rangle + V_{43}|-,+,-,n_1+1,0\rangle + V_{53}|-,-,+,n_1+1,0\rangle + V_{63}|-,-,-,n_1+1,1\rangle\Big] + \sin\alpha\Big[U_{16}|+,+,+,n_1-1,0\rangle + U_{26}|+,+,-,n_1-1,1\rangle + U_{36}|+,-,+,n_1-1,1\rangle + U_{46}|-,+,+,n_1,0\rangle + U_{56}|+,-,-,n_1-1,2\rangle + U_{66}|-,+,-,n_1,1\rangle + U_{76}|-,-,+,n_1,1\rangle + U_{86}|-,-,-,n_1,2\rangle\Big].$$

5) Case $n_1 = 0$, $n_2 \geq 2$ $\big(U_{ij} = U_{ij}(0,n_2-2,t), V_{ij} = V_{ij}(n_2-1,t)\big)$:

$$|\psi_{0_1n_2}(t)\rangle = \cos\alpha\Big[U_{15}|+,+,+,0,n_2-2\rangle + U_{25}|+,+,-,0,n_2-1\rangle + U_{35}|+,-,+,0,n_2-1\rangle + U_{45}|-,+,+,1,n_2-2\rangle + U_{55}|+,-,-,0,n_2\rangle + U_{65}|-,+,-,1,n_2-1\rangle + U_{75}|-,-,+,1,n_2-1\rangle + U_{85}|-,-,-,1,n_2\rangle\Big] + \sin\alpha\Big[V_{78}|-,+,+,0,n_2-1\rangle + V_{88}|-,+,-,0,n_2\rangle + V_{98}|-,-,+,0,n_2\rangle + V_{10,8}|-,-,-,0,n_2+1\rangle\Big].$$

6) Case $n_1 \geq 1$, $n_2 \geq 2$ $\big(U_{i5} = U_{i5}(n_1,n_2-2,t), U_{i6} = U_{i6}(n_1-1,n_2-1,t)\big)$:

$$|\psi_{n_1n_2}(t)\rangle = \cos\alpha\Big[U_{15}|+,+,+,n_1,n_2-2\rangle + U_{25}|+,+,-,n_1,n_2-1\rangle + U_{35}|+,-,+,n_1,n_2-1\rangle + U_{45}|-,+,+,n_1+1,n_2-2\rangle + U_{55}|+,-,-,n_1,n_2\rangle + U_{65}|-,+,-,n_1+1,n_2-1\rangle + U_{75}|-,-,+,n_1+1,n_2-1\rangle + U_{85}|-,-,-,n_1+1,n_2\rangle\Big] + \sin\alpha\Big[U_{16}|+,+,+,n_1-1,n_2-1\rangle + U_{26}|+,+,-,n_1-1,n_2\rangle + U_{36}|+,-,+,n_1-1,n_2\rangle + U_{46}|-,+,+,n_1,n_2-1\rangle + U_{56}|+,-,-,n_1-1,n_2+1\rangle + U_{66}|-,+,-,n_1,n_2\rangle + U_{76}|-,-,+,n_1,n_2\rangle + U_{86}|-,-,-,n_1,n_2+1\rangle\Big].$$

Having solved the problem of searching for the wave function $|\psi_{n_1 n_2}(t)\rangle$ at subsequent time points $t > 0$ for the Fock states of resonator fields, we can proceed to determine the time density matrix of the considered model for the initial states of qubits (10)–(14) in case of initial single-mode thermal states of the resonator fields, the density matrix of which is expressed by the formula: $\hat{\wp}_{F_l}(0) = \sum_{n_l} p_{n_l} |n_l\rangle\langle n_l|$, where $l = 1, 2$. Here, the statistical weights p_{n_l} are expressed by the following formula: $p_{n_l} = \bar{n}_l^{n_l}/(\bar{n}_l + 1)^{n_l+1}$, where $\bar{n}_l$ — is the average number of thermal photons in the corresponding resonator, which is determined by the standard Bose–Einstein formula $\bar{n}_l = (\exp[\hbar\omega_c/k_B T_l] - 1)^{-1}$. Here k_B — Boltzmann constant, T_l — temperature of the appropriate resonator.

To generalize the results for the case of resonators thermal fields, it is necessary to solve the quantum Liouville equation.

$$i\hbar \frac{\partial \hat{\wp}_{ABCF_1F_2}(t)}{\partial t} = [\hat{H}_{Int}, \hat{\wp}_{ABCF_1F_2}(t)], \qquad (15)$$

i.e. find the density matrix of the full system $\hat{\wp}_{ABCF_1F_2}(t)$. Knowing the explicit form of $|\psi_{n_1 n_2}(t)\rangle$ wave functions at subsequent $t > 0$ time points in case of the Fock states of resonator fields, the density matrix can be calculated as follows:

$$\hat{\wp}_{ABCF_1F_2}(t) = \sum_{n_1=0}^{\infty}\sum_{n_2=0}^{\infty} p_{n_1} p_{n_2} |\psi_{n_1 n_2}(t)\rangle\langle\psi_{n_1 n_2}(t)|. \qquad (16)$$

For the states (10), (13), (14) the full density matrix will be written as follows :

$$\hat{\wp}_{ABCF_1F_2}(t) = \sum_{n_1=1}^{\infty}\sum_{n_2=2}^{\infty} p_{n_1} p_{n_2} |\psi_{n_1 n_2}(t)\rangle\langle\psi_{n_1 n_2}(t)|$$
$$+ p_{0_1} \sum_{n=2}^{\infty} p_{n_2} |\psi_{0_1 n_2}(t)\rangle\langle\psi_{0_1 n_2}(t)|$$
$$+ p_{1_2} \sum_{n_1=1}^{\infty} p_{n_1} |\psi_{n_1 1_2}(t)\rangle\langle\psi_{n_1 1_2}(t)|$$
$$+ p_{0_2} \sum_{n_1=1}^{\infty} |\psi_{n_1 0_2}(t)\rangle\langle\psi_{n_1 0_2}(t)| + p_{0_1} p_{1_2} |\psi_{0_1 1_2}(t)\rangle\langle\psi_{0_1 1_2}(t)|$$
$$+ p_{0_1} p_{0_2} |\psi_{0_1 0_2}(t)\rangle\langle\psi_{0_1 0_2}(t)|,$$

and for the states (11), (12) it is written as

$$\hat{\wp}_{ABCF_1F_2}(t) = \sum_{n_1=1}^{\infty}\sum_{n_2=1}^{\infty} p_{n_1} p_{n_2} |\psi_{n_1 n_2}(t)\rangle\langle\psi_{n_1 n_2}(t)|$$
$$+ p_{0_1} \sum_{n_2=1}^{\infty} p_{n_2} |\psi_{0_1 n_2}(t)\rangle\langle\psi_{0_1 n_2}(t)|$$
$$+ p_{0_2} \sum_{n_1=1}^{\infty} p_{n_1} |\psi_{n_1 0_2}(t)\rangle\langle\psi_{n_1 0_2}(t)| + p_{0_1} p_{0_2} |\psi_{0_1 0_2}(t)\rangle\langle\psi_{0_1 0_2}(t)|.$$

Thus, using solutions for the Fock states of resonator fields, labor-intensity calculations can be used to generalize the results to the case of resonator fields thermal states (16) and solve the quantum Liouville equation (15).

To study the evolution of the subsystem of qubits, we need to calculate reduced three- and two-qubit density matrices, which are related to the full density matrix (16) using the operation of taking a trace over the variables of all fields and/or qubits as follows: $\hat{\wp}_{ABC}(t) = \mathrm{Tr}_{F_1}\mathrm{Tr}_{F_2}\hat{\wp}_{ABCF_1F_2}(t)$, $\hat{\wp}_{ij}(t) = \mathrm{Tr}_k \hat{\wp}_{ABC}(t)$ respectively. Here, the indices have the following values: $i, j, k = A, B, C$ and $i \neq j \neq k$ is fulfilled.

2. Selection of entanglement criteria for the investigated model and their calculation

In this paper, we analyze three-qubit and two-qubit entanglements in detail. To study the three-qubit entanglement of initial states (12)–(14), as a criterion we use the fidelity Φ, which is expressed as follows [26]:

$$\Phi(t) = \mathrm{Tr}(\hat{\wp}_{ABC}(0)\hat{\wp}_{ABC}(t)). \qquad (17)$$

Thus, the fidelity Φ shows how much the three-qubit state at any given time $t > 0$ coincides with the original three-qubit state. In the case of biseparable initial states (10), (11), the fidelity Φ is not informative. We omit the detailed output of expressions for the fidelity (17) through the elements of the three-qubit density matrix $\hat{\wp}_{ABC}$ to save space and immediately provide the final expressions for the initial states (12)–(14):

$$\Phi = A^2\wp_{22} + B^2\wp_{33} + C^2\wp_{44} + 2AB\,\mathrm{Re}\,\wp_{23}$$
$$+ 2AC\,\mathrm{Re}\,\wp_{24} + 2BC\,\mathrm{Re}\,\wp_{34},$$

$$\Phi = C^2\wp_{55} + B^2\wp_{66} + A^2\varrho_{77} + 2AC\,\mathrm{Re}\,\wp_{57}$$
$$+ 2AB\,\mathrm{Re}\,\wp_{67} + 2BC\,\mathrm{Re}\,\wp_{56},$$

$$\Phi = \cos^2\vartheta\,\wp_{11} + \sin^2\vartheta\,\wp_{88} + 2\cos\vartheta\sin\vartheta\,\mathrm{Re}\,\wp_{18},$$

respectively. Here, the variables $A = \cos\theta$, $B = \sin\theta\sin\varphi$, $C = \sin\theta\cos\varphi$ are introduced. As an example, we write down the elements of the three-qubit density matrix $\hat{\wp}_{ABC}$, which are used in calculating the fidelity Φ, for the state (14):

$$\wp_{11} = \sin^2\vartheta \sum_{n_1=1}^{\infty}\sum_{n_2=2}^{\infty} p_{n_1} p_{n_2} |U_{18}|^2 + \cos^2\vartheta \sum_{n_1=0}^{\infty}\sum_{n_2=0}^{\infty} p_{n_1} p_{n_2} |U_{11}|^2,$$

$$\wp_{88} = \sum_{n_1=1}^{\infty}\sum_{n_2=2}^{\infty} p_{n1}p_{n_2}\left[\cos^2\vartheta|U_{81}|^2 + \sin^2\vartheta|U_{88}|^2\right]$$

$$+ p_{0_1}\sum_{n_2=2}^{\infty} p_{n_2}\left[\cos^2\vartheta|U_{81}|^2 + \sin^2\vartheta V_{10,10}\right]$$

$$+ p_{1_2}\sum_{n_1=1}^{\infty} p_{n_1}\left[\cos^2\vartheta|U_{81}|^2 + \sin^2\vartheta|V_{66}|^2\right]$$

$$+ p_{0_2}\sum_{n_1=1}^{\infty} p_{n_1}\left[\cos^2\vartheta|U_{81}|^2 + \sin^2\vartheta|S_{22}|^2\right]$$

$$+ p_{0_1}p_{1_2}\left[\cos^2\vartheta|U_{81}|^2 + \sin^2\vartheta|S_{55}|^2\right]$$

$$+ p_{0_1}p_{0_2}\left[\cos^2\vartheta|U_{81}|^2 + \sin^2\vartheta\right],$$

$$\wp_{18} = \cos\vartheta\sin\vartheta\left\{\sum_{n_1=1}^{\infty}\sum_{n_2=2}^{\infty} p_{n_1}p_{n_2}U_{11}U_{88}^* + p_{0_1}\sum_{n_2=2}^{\infty} p_{n_2}U_{11}\right.$$

$$\times V_{10,10}^* + p_{1_2}\sum_{n_1=1}^{\infty} p_{n_1}U_{11}V_{66}^* + p_{0_2}\sum_{n_1=1}^{\infty} p_{n_1}U_{11}S_{22}^*$$

$$\left. + p_{0_1}p_{1_2}U_{11}S_{55}^* + p_{0_1}p_{0_2}U_{11}\right\}.$$

where the following notation is introduced

$$U_{i1} \equiv U_{i1}(n_1, n_2, t),$$

$$U_{i8} \equiv U_{i8}(n_1 - 1, n_2 - 2, t),$$

$$V_{10,10} \equiv V_{10,10}(n_2 - 2, t),$$

$$V_{66} \equiv V_{66}(n_1 - 1, t),$$

$$S_{22} \equiv S_{22}(n_1 - 1, t),$$

$$S_{55} \equiv S_{55}(t)$$

with the appropriate numbers of photons n_1 and n_2 in resonators.

When studying the qubits entanglement dynamics in the considered model for the biseparable and genuine entangled W-type states, we will use the criterion of negativity of pairs of qubits as a quantitative criterion of entanglement. Negativity criterion of two qubits i and j may be expressed as [27]:

$$\xi_{ij} = -2\sum_k (\lambda_{ij})_k^-, \tag{18}$$

where λ_{ij} — are all possible negative eigenvalues of the two-qubit density matrix $\hat{\wp}_{ij}^{\mathrm{T}}(t)$, on which a partial transpose operation was performed with respect to the variables of the first qubit. The two-qubit density matrix $\hat{\wp}_{ij}^{\mathrm{T}}(t)$ has the following form for the initial biseparable states (10), (11) and the initial W-states (12), (13):

$$\hat{\wp}_{ij}^{\mathrm{T}}(t) = \begin{pmatrix} \wp_{11}^{ij} & 0 & 0 & \wp_{32}^{ij} \\ 0 & \wp_{22}^{ij} & 0 & 0 \\ 0 & 0 & \wp_{33}^{ij} & 0 \\ \wp_{23}^{ij} & 0 & 0 & \wp_{44}^{ij} \end{pmatrix}, \begin{pmatrix} |+_i, +_j\rangle \\ |+_i, -_j\rangle \\ |-_i, +_j\rangle \\ |-_i, -_j\rangle \end{pmatrix} \longleftrightarrow \begin{pmatrix} 1 \\ 2 \\ 3 \\ 4 \end{pmatrix}.$$

The negativity will be written as follows

$$\xi_{ij} = \sqrt{(\wp_{44}^{ij} - \wp_{11}^{ij})^2 + 4|\wp_{23}^{ij}|^2} - \wp_{11}^{ij} - \wp_{44}^{ij}.$$

As an example, we write down the elements of the two-qubit density matrix (19), which are used to calculate the negativity (18) in case of A and B qubits, for the initial state of the qubits (12):

$$\wp_{11}^{AB} = \sum_{n_1=1}^{\infty} p_{n_1}\sum_{n_2=1}^{\infty} p_{n_2}\left\{\left[AU_{12} + BU_{13}\right]\left[AU_{12}^* + BU_{13}^*\right]\right.$$

$$\left. + \left[AU_{22} + BU_{23}\right]\left[AU_{22}^* + BU_{23}^*\right] + C^2\left[|U_{14}|^2 + |U_{24}|^2\right]\right\}$$

$$+ p_{0_1}\sum_{n_2=1}^{\infty} p_{n_2}\left\{\left[AU_{12} + BU_{13}\right]\left[AU_{12}^* + BU_{13}^*\right]\right.$$

$$\left. + \left[AU_{22} + BU_{23}\right]\left[AU_{22}^* + BU_{23}^*\right]\right\}$$

$$+ p_{0_2}\sum_{n_1=1}^{\infty} p_{n_1}\left\{\left[AV_{11} + BV_{12}\right]\left[AV_{11}^* + BV_{12}^*\right]\right.$$

$$\left. + C^2\left[|U_{14}|^2 + |U_{24}|^2\right]\right\} + p_{0_1}p_{0_2}\left[AV_{11} + BV_{12}\right]$$

$$\times\left[AV_{11}^* + BV_{12}^*\right],$$

$$\wp_{23}^{AB} = C\left\{\sum_{n_1=1}^{\infty} p_{n_1}\sum_{n_2=1}^{\infty} p_{n_2}\left[\left(AU_{32} + BU_{33}\right)U_{44}^*\right.\right.$$

$$\left. + \left(AU_{52} + BU_{53}\right)U_{64}^*\right] + p_{0_1}\sum_{n_2=1}^{\infty} p_{n_2}\left[\left(AU_{32} + BU_{33}\right)V_{77}^*\right.$$

$$\left. + \left(AU_{52} + BU_{53}\right)V_{87}^*\right] + p_{0_2}\sum_{n_1=1}^{\infty} p_{n_1}\left[\left(AV_{21} + BV_{22}\right)U_{44}\right.$$

$$\left. + \left(AV_{31} + BV_{32}\right)U_{64}\right] + p_{0_1}p_{0_2}\left[\left(AV_{21} + BV_{22}\right)V_{77}^*\right.$$

$$\left.\left. + \left(AV_{31} + BV_{32}\right)V_{87}^*\right]\right\},$$

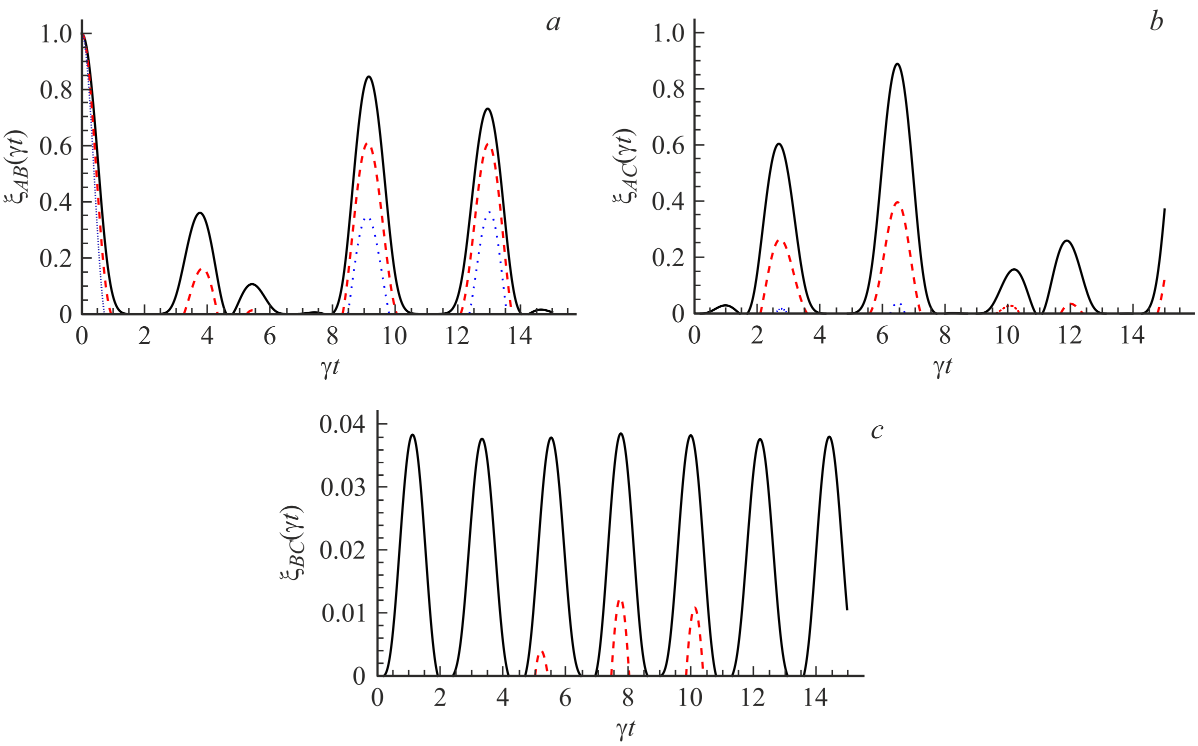

Figure 2. Negativity criterion $\varepsilon_{ij}(\gamma t)$ for i- and j-qubits versus reduced time γt for the initial state of qubits (10) in case $\alpha = \pi/4$. Intensity of thermal fields: $\bar{n}_1 = \bar{n}_2 = 0.01$ (black solid line), $\bar{n}_1 = \bar{n}_2 = 0.2$ (red dashed line), $\bar{n}_1 = \bar{n}_2 = 0.5$ (blue dotted line).

$$\wp_{44}^{AB} = \sum_{n_1=1}^{\infty} p_{n_1} \sum_{n_2=1}^{\infty} p_{n_2} \Big\{ \Big[AU_{72} + BU_{73}\Big] \Big[AU_{72}^* + BU_{73}^*\Big]$$

$$+ \Big[AU_{82} + BU_{83}\Big] \Big[AU_{82}^* + BU_{83}^*\Big] + C^2 \Big[|U_{74}|^2 + |U_{84}|^2\Big] \Big\}$$

$$+ p_{0_1} \sum_{n_2=1}^{\infty} p_{n_2} \Big\{ \Big[AU_{72} + BU_{73}\Big] \Big[AU_{72}^* + BU_{73}^*\Big]$$

$$+ \Big[AU_{82} + BU_{83}\Big] \Big[AU_{82}^* + BU_{83}^*\Big] + C^2 \Big[|V_{97}|^2 + |V_{107}|^2\Big] \Big\}$$

$$+ p_{0_2} \sum_{n_1=1}^{\infty} p_{n_1} \Big\{ \Big[AV_{51} + BV_{52}\Big] \Big[AV_{51}^* + BV_{52}^*\Big]$$

$$+ \Big[AV_{61} + BV_{62}\Big] \Big[AV_{61}^* + BV_{62}^*\Big] + C^2 \Big[|U_{74}|^2 + |U_{84}|^2\Big] \Big\}$$

$$+ p_{0_1} p_{0_2} \Big\{ \Big[AV_{51} + BV_{52}\Big] \Big[AV_{51}^* + BV_{52}^*\Big] + \Big[AV_{61} + BV_{62}\Big]$$

$$\times \Big[AV_{61}^* + BV_{62}^*\Big] + C^2 \Big[|V_{97}|^2 + |V_{107}|^2\Big] \Big\},$$

where the following notation is introduced

$$U_{i2(i3)} \equiv U_{i2(i3)}(n_1, n_2 - 1, t),$$

$$U_{i4} \equiv U_{i4}(n_1 - 1, n_2, t),$$

$$V_{k1(k2)} \equiv V_{k1(k2)}(n_1, t),$$

$$V_{j7} \equiv V_{j7}(n_2, t)$$

with the appropriate number of n_1 and n_2 photons in resonators $(i = 1, 2, \ldots 8,\ \ k = 1, 2, \ldots 6,\ \ j = 1, 2, 3, 4)$. The remaining elements of the two-qubit density matrix are not given here to save space because these expressions are too large.

3. Results of computational modelling and discussion

Figure 2 shows the dynamics of $\xi_{ij}(\gamma t)$ negativity criterion for different pairs of i and j qubits from γt scalable time for different values of the average number of thermal photons in both resonators provided $\bar{n}_1 = \bar{n}_2$ for the initial biseparable three-qubit state (10). All graphs are plotted provided that A and B qubits are at the initial moment of time $t = 0$ in the maximally entangled Bell state $(\xi_{AB}(0) = 1)$, i.e. the initial entanglement parameter is set to $\alpha = \pi/4$. It is clearly seen from Fig. 2, *a* that the initial Bell entanglement quickly collapses even at sufficiently low field intensities of resonators $(\bar{n}_1 \to 0$ and $\bar{n}_2 \to 0)$, since negativity never assumes its initial value during evolution $(\xi_{AB}(t) \neq 1)$ and, moreover, negativity regularly assumes zero values, which means about the presence of the parasitic effect of sudden death of entanglement. The qubits A and C and B and C at the initial moment of time were in the non-entangled state, which is fully agreeable with Fig. 2, *b, c*. However, in the process of evolution, thermal fields of the resonators induce entanglement of varying degrees between

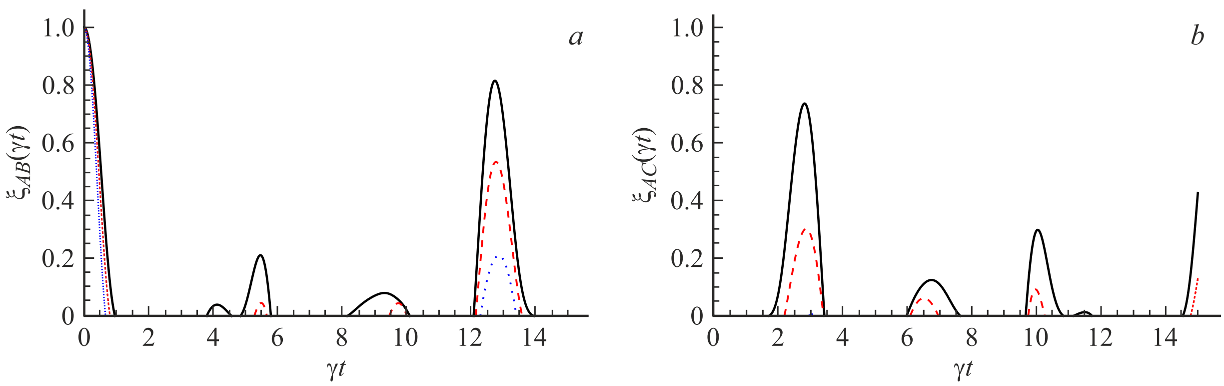

Figure 3. Similar in Fig. 2, but for the initial state of qubits (11) in case $\alpha = \pi/4$.

these pairs of qubits. This effect was predicted earlier for the two-qubit systems. The A and B qubits have the most stable entanglement with respect to the thermal fields of the resonators, since even for a relatively large average number of thermal photons $\bar{n}_1 = \bar{n}_2 = 0.5$, entanglement is observed at some time intervals. On the contrary, the qubits B and C are slightly entangled during evolution, since the pairwise negativity does not exceed $\xi_{BC}(\gamma t) \leq 0.04$ over the entire time interval, which is a rather interesting result.

In Fig. 3, we plot the curves similar to those shown in Fig. 2, but for a biseparable three-qubit state (11). In general, the results for the state (11) coincide with the conclusions for the biseparable state (10), but there are a number of fundamental differences. First, the entanglement between B and C qubits is not induced even for the vacuum resonator fields, i.e. in case of $n_1 = n_2 = 0$. Second, the degree of entanglement between pairs of A and B and A and C qubits at subsequent $t > 0$ time points for the initial biseparable state (11) is much less than the degree of pairwise entanglement for the biseparable state (10). Third, higher intensity of resonators thermal fields $\bar{n}_1$, $\bar{n}_2$ significantly reduces the maximum degree of entanglement of qubits much faster in the case of a biseparable state of qubits (11). Thus, the initial state of the qubits (11) is extremely sensitive to the thermal noise of resonators. Note that the above conclusions for biseparable states (10), (11) are quite different from the results for the model with three qubits in a common resonator, which we studied earlier in [25].

In Fig. 4, 5 we demonstrate the results of computational modeling for the negativity criterion ξ_{AB} or ξ_{AC} (a), ξ_{BC} (b) and fidelity Φ depending on the reduced time γt for the genuine entangled three-qubit W-state (12) and (13) in case $\theta = \arccos(1/\sqrt{3})$, $\varphi = \pi/4$. These initial entanglement parameters θ and φ were selected because at the specified values, the W-states (12) and (13) enter the most symmetrical state, i.e. for all pairs of qubits, the negativity criterion takes a value equal to $\xi_{ij}(0) = (\sqrt{5} - 1)/3$. The graphs clearly show that higher intensities of the resonators' thermal fields $\bar{n}_1$ and $\bar{n}_2$ result in a significant decrease in the maximum degree of pairwise entanglement of qubits for both W-states. It should be emphasized that the reduction in the degree of pairwise entanglement of qubits occurs much faster in this model than with three qubits in a common resonator [25]. Moreover, in this model, the fildeity Φ never returns to its initial value ($\Phi(\gamma t) \neq 1$) for both W-states (12), (13) even in case of resonators' vacuum fields $\bar{n}_1 \to 0$, $\bar{n}_2 \to 0$ which is fundamentally different from the three-qubit models studied earlier [22–25]. An interesting result is also that the pairwise entanglement of B and C qubits in case of W-state (12) may exceed at some time the initial value of the negativity criterion $\xi_{BC} \geq (\sqrt{5} - 1)/3$, which is not observed for the second W-state (13). It is also worth noting that for a given pair of B and C qubits, at any intensity of thermal fields of resonators $\bar{n}_1$ and $\bar{n}_2$, the regions with the effect of sudden death of entanglement are much smaller for the second W-state (13) than for the first W-state (12).

Finally, in Fig. 6, we demonstrate the fildeity Φ versus scaled time γt for different intensities of thermal fields of resonators $\bar{n}_1$ and $\bar{n}_2$ for the initial GHZ state (14) in case of $\vartheta = \pi/4$. As for W-states (12)–(13), the resonators thermal noise significantly reduces the maximum value of the fildeity Φ and, moreover, three qubits at subsequent time points t never return to the initial GHZ state (14) even in case of vacuum fields of resonators $\bar{n}_1 \to 0$, $\bar{n}_2 \to 0$. Calculations show that the pairwise negativity ξ_{ij} in case of GHZ state (14) has zero values over the entire time interval at any intensity of thermal fields of resonators $\bar{n}_1$ and $\bar{n}_2$. Additional computer modeling also shows that all of the above conclusions are valid for the initial states (10)–(14) at different initial entanglement parameters α, θ, φ and ϑ. Note the rather complex behavior of the entanglement parameters ξ_{ij}, Φ for all initial three-qubit states (10)–(14) at any resonator intensities $\bar{n}_1$ and $\bar{n}_2$, which does not allow for a detailed analysis of the behavior of the negativity criterion ξ_{ij} and the fildeity Φ for vacuum resonator fields. This result is fundamentally different from the results we obtained for other types of three-qubit models [22–25]. This is explained by the different dynamics of A qubit in the first resonator and B and C qubits in the second resonator. The mentioned dynamics of qubits

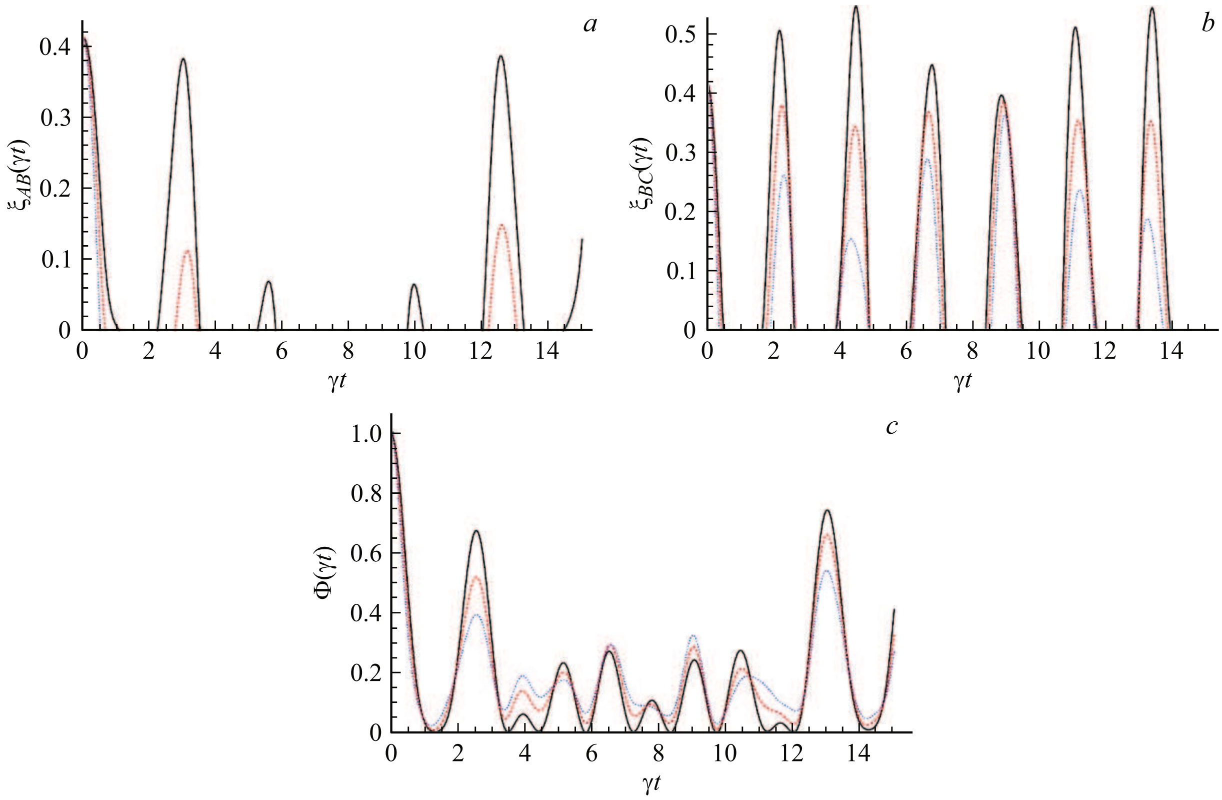

Figure 4. Dependence of the negativity criterion $\varepsilon_{ij}(\gamma t)$ for i and j-qubits and fidelity Φ of three qubits on the reduced time γt for the initial state of qubits (12) in case of $\theta = \arccos(1/\sqrt{3})$, $\varphi = \pi/4$. Intensity of thermal fields: $\bar{n}_1 = \bar{n}_2 = 0.01$ (black solid line), $\bar{n}_1 = \bar{n}_2 = 0.2$ (red dashed line), $\bar{n}_1 = \bar{n}_2 = 0.5$ (blue dotted line).

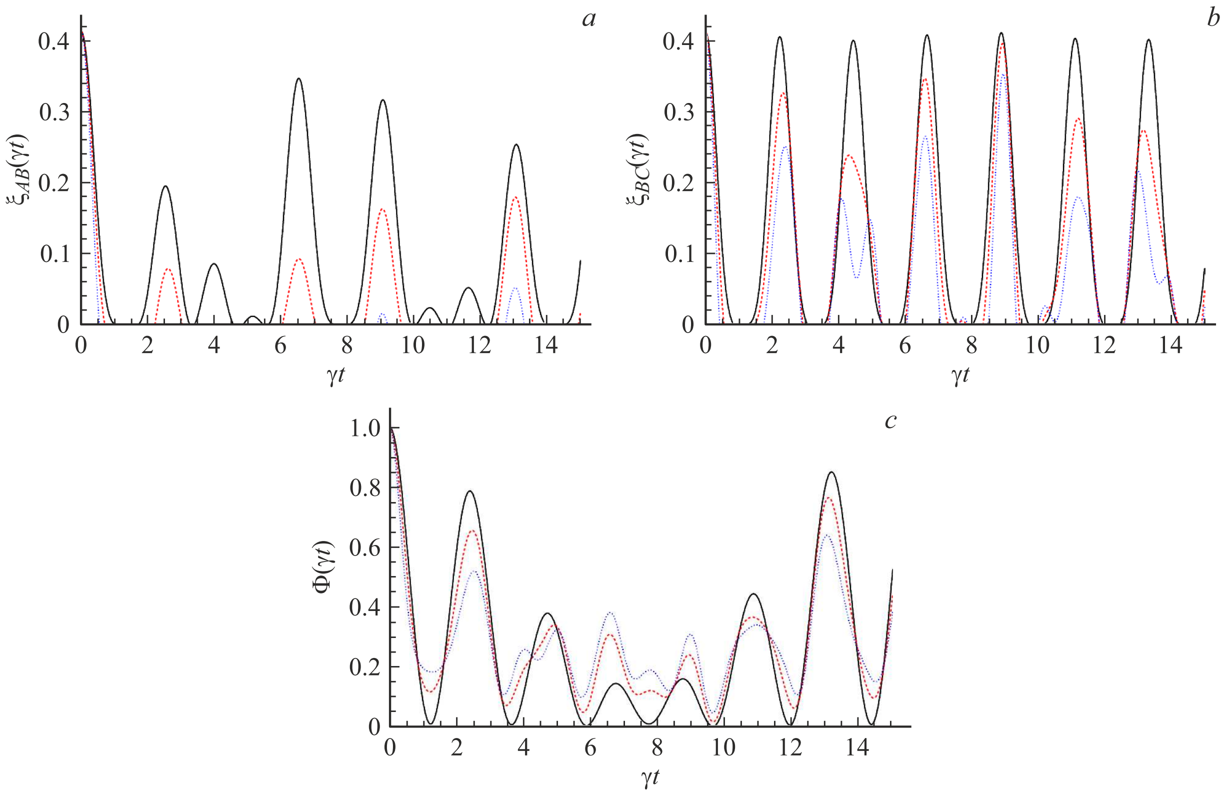

Figure 5. Similar, in Fig. 4, but for the initial state of qubits (13) in case $\theta = \arccos(1/\sqrt{3})$, $\varphi = \pi/4$.

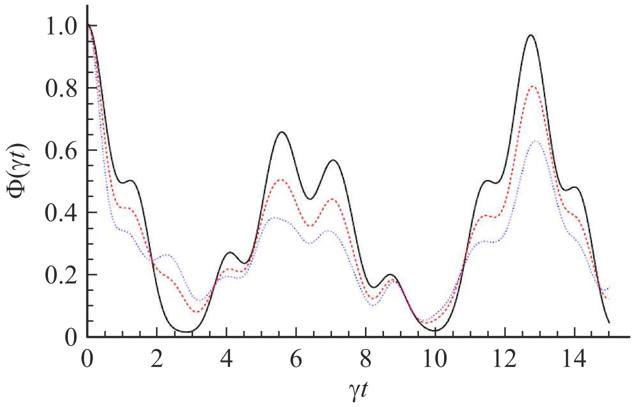

Figure 6. Fidelity Φ versus reduced time γt for the initial state of qubits (14) in case of $\vartheta = \pi/4$. Intensity of thermal fields: $\bar{n}_1 = \bar{n}_2 = 0.01$ (black solid line), $\bar{n}_1 = \bar{n}_2 = 0.2$ (red dashed line), $\bar{n}_1 = \bar{n}_2 = 0.5$ (blue dotted line).

in case of vacuum fields of resonators $n_1 = n_2 = 0$ can be studied by analyzing the population inversion of one $W_j = \wp^j_{11} - \wp^j_{22}$ qubit, determined through the elements of the corresponding one-qubit density matrix $\hat{\wp}_j$, and the time wave function $|\psi_{n_1 n_2}(t)\rangle$. A detailed analysis of population inversion dynamics in case of vacuum fields of resonators $n_1 = n_2 = 0$ due to their bulkiness will be presented in our next paper.

Conclusion

Thus, in our work we found an exact expression for the evolution operator for a new three-particle model consisting of one Jaynes-Cummings qubit and two Tavis-Cummings qubits trapped in independent ideal high-Q resonators and resonantly interacting with the corresponding selected quantum modes of these resonators. With its help, an exact solution of the quantum Liouville equation was found for the thermal states of resonator fields and various states of qubits: biseparable and genuine entangled W- and GHZ-states. Using reduced qubit density matrices, we calculated two entanglement parameters: the pairwise negativity ξ_{ij} and the fidelity Φ. As a result, we have shown that qubits in the process of evolution do not return to their initial states at any intensity of thermal fields of resonators $\bar{n}_1$ and $\bar{n}_2$, which fundamentally distinguishes the behavior of the studied model from the behavior of the previously considered three-qubit models [22–25]. For qubits trapped in various resonators and initially being in the entangled state, the effect of sudden death and recovery of pairwise entanglement occurs throughout the entire time of evolution for a fairly wide range of thermal intensities $\bar{n}_1$ and $\bar{n}_2$. However, a significant deviation of thermal fields intensities of $\bar{n}_1$ and $\bar{n}_2$ resonators from the vacuum states rather quickly leads to complete decoherence of entanglement for all pairs of qubits and to the absence of any recovery of pairwise entanglement of qubits. At the same time, in the previously studied three-qubit models [22–25], the maximum degree of pairwise entanglement of qubits and the fidelity in time for the same values of resonator field intensities declined much slower. We also note a significantly more complex temporal behavior of the entanglement parameters in comparison with the previously considered three-qubit models, even for the vacuum fields of resonators $\bar{n}_1 \to 0$, $\bar{n}_2 \to 0$, which does not allow for a detailed analysis of the qubits dynamics and the calculation of the oscillation period of Rabi oscillations in an analytical form. Overall, this study significantly improves our understanding of the key features of the qubit entanglement dynamics in the considered three-particle model.

Funding

The study was supported as part of the state assignment of the Ministry of Science and Higher Education of the Russian Federation, №FSSS-2025-0003.

Conflict of interest

The authors declare that they have no conflict of interest.

References

[1] M.A. Nielsen, I.L. Chuang. *Quantum Computation and Quantum Information.* 10th Anniversary Edition (Cambridge University Press: NY., USA, 2010), 702 p. DOI: 10.1017/CBO9780511976667
[2] A. Barenco et al. Phys. Rev. A, **52**, 3457 (1995). DOI: 10.1103/PhysRevA.52.3457
[3] Y. Shi. Quantum Information and Computation, **3**, 84 (2003).
[4] E. Barnes, C. Arenz, A.J.G. Pitchford, S.E. Economou. Phys. Rev. B, **96** (2), 024504 (2017). DOI: 10.1103/PhysRevB.96.024504
[5] M. Li, L. Jia, J. Wang, S. Shen, S.M. Fei. Phys. Rev. A, **96**, 052314 (2017). DOI: 10.1103/PhysRevA.96.052314
[6] M.D. Reed, L. DiCarlo, S.E. Nigg, L. Sun, L. Frunzio, S.M. Girvin, R.J. Schoelkopf. Nature, **482**, 382 (2012). DOI: 10.1038/nature10786
[7] A. Isar. Open Systems Information Dynamics, **16** (2), 205 (2009). DOI: 10.1142/S1230161209000153
[8] L. Aolita, R. Chaves, D. Cavalcanti, A. Acin, L. Davidovich. Phys. Rev. Lett., **100** (8), 080501 (2008). DOI: 10.1103/PhysRevLett.100.080501
[9] Z.-L. Xiang, S. Ashhab, J.Q. You, F. Nori. Rev. Mod. Phys., **85**, 623 (2013). DOI: 10.1103/revmodphys.85.623
[10] I.M. Georgescu, S. Ashhab, F. Nori. Rev. Mod. Phys., **86**, 153 (2014). DOI: 10.1103/RevModPhys.86.153
[11] G. Wendin. Rep. Prog. Phys., **80** (10), 106001 (2017). DOI: 10.1088/1361-6633/aa7e1a
[12] G.-Q. Li, X.-Y. Pan. Chin. Phys. B, **27** (2), 020304 (2018). DOI: 10.1088/1674-1056/27/2/020304
[13] D.J. van Woerkom, P. Scarlino, J.H. Ungerer, C. Muller, J.V. Koski, A.J. Landig, C. Reichl, W. Wegscheider, T. Ihn, K. Ensslin, A. Wallraff. Phys. Rev. X, **8**, 041018 (2018). DOI: 10.1103/PhysRevX.8.041018
[14] B.W. Shore, P.L. Knight. J. Mod. Opt., **40** (7), 1195 (1993). DOI: 10.1080/09500349314551321

[15] J. Larson, T. Mavrogordatos. *The Jaynes-Cummings Model and Its Descendants: Modern research directions.* (IoP Publishing, Bristol 2021), 426 p. DOI: 10.1088/978-0-7503-3447-1
[16] M. Neeley, R.C. Bialczak, M. Lenander, E. Lucero, M. Mariantoni, A.D. O'Connell, D. Sank, H. Wang, M. Weides, J. Wenner, Y. Yin, T. Yamamoto, A.N. Cleland, J.M. Martinis. Nature, **467**, 570 (2010). DOI: 10.1038/nature09418
[17] L. DiCarlo, M.D. Reed, L. Sun, B.R. Johnson, J.M. Chow, J.M. Gambetta, L. Frunzio, S.M. Girvin, M.H. Devoret, R.J. Schoelkopf. Nature, **467**, 574 (2010). DOI: 10.1038/nature09416
[18] Ch.F. Roos, M. Riebe, H. Höffner, W. Hönsel, J. Benhelm, G.P.T. Lancaster, Ch. Becher, F. Schmidt-Kaler, R. Blatt. Nature, **429**, 734 (2004). DOI: 10.1038/nature02570
[19] D.C. Cole, J.J. Wu, S.D. Erickson, P.-Y. Hou, A.C. Wilson, D. Leibfried, F. Reiter. New J. Phys., **23**, 073001 (2021). DOI: 10.1088/1367-2630/ac09c8
[20] P. Neumann, N. Mizuochi, F. Rempp, P. Hemmer, H. Watanabe, S. Yamasaki, V. Jacques, T. Gaebel, F. Jelezko, J. Wrachtrup. Science, **320**, 1326 (2008). DOI: 10.1126/science.1157233
[21] K. Takeda, A. Noiri, T. Nakajima, J. Yoneda, T. Kobayashi, S. Tarucha. Nature Nanotechnol., **16**, 965 (2021). DOI: 10.1038/s41565-021-00925-0
[22] A.R. Bagrov, E.K. Bashkirov. ZhTF, **94** (3), 341 (2024) (in Russian). DOI: 10.61011/JTF.2024.03.57370.301-23
[23] A.R. Bagrov, E.K. Bashkirov. ZhTF, **95** (5), 853 (2025) (in Russian). DOI: 10.61011/JTF.2025.05.60275.433-24
[24] E.K. Bashkirov, A.R. Bagrov. Quantum Inf. Process., **24** (5), 154 (2025). DOI: 10.1007/s11128-025-04772-z
[25] E.K. Bashkirov, A.R. Bagrov. Laser Phys., **35** (6), 065203 (2025). DOI: 10.1088/1555-6611/addd90
[26] R. Jozsa. J. Mod. Opt., **41**, 2315 (1994). DOI: 10.1080/09500349414552171
[27] A. Peres. Phys. Rev. Lett., **77** (8), 1413 (1996). DOI: 10.1103/PhysRevLett.77.1413

Translated by T.Zorina

Translated by T.Zorina